

# DISTANCE-TIME AUTOCORRELATION FUNCTIONS FOR WINDS IN THE AUSTRALIAN REGION

551.501.75:

551.553

R. S. Seaman

Australian Numerical Meteorology Research Centre, Melbourne

(Manuscript received June 1975)

## ABSTRACT

Distance-time autocorrelation functions have been fitted to zonal and meridional correlation coefficients of wind from 51 station pairs over Australia for time lags up to 24 hours, at 500 and 200 mb in summer and winter. Functions based on geostrophic flow in a horizontally homogeneous and isotropic atmosphere explain about 85 per cent of the data variance, although some systematic discrepancies are apparent. The centres of maximum correlation move at a velocity much less than that predicted by frozen turbulence, and the meridional maximum decreases more rapidly with increasing lag than does the zonal maximum. The functions indicate a systematic variation of this velocity with season and latitude, but not with level.

## INTRODUCTION

The variability of wind with distance and time on an isobaric surface may be described by correlation coefficients relating zonal and meridional components ( $u, v$ ) and ( $u', v'$ ) at pairs of points  $P$  and  $P'$  for various time lags. Buell (1971) has shown that the correlation coefficients  $r_{uu'}$  and  $r_{vv'}$  predominate over  $r_{uv'}$  and  $r_{vu'}$ , although the latter two are not negligible. Using Australian upper wind soundings from 1962 to 1972, Seaman and Draudins (1975) computed  $r_{uu'}$  and  $r_{vv'}$  (subsequently denoted as  $r_u$  and  $r_v$ ) for 51 station pairs at seven time lags from -24 to +24 hours in summer and winter, at levels approximating the 500 mb and 200 mb isobaric surfaces. The purpose of this report is to describe the systematic behaviour of  $r_u$  and  $r_v$  by means of autocorrelation functions (acfs)  $r_u(x, y, t)$  and  $r_v(x, y, t)$ , where  $x, y$  and  $t$  are the zonal and meridional separations and time lags between station pairs. Some differences between components, seasons, levels and geographical areas will be discussed.

## FACTORS INFLUENCING CHOICE OF AUTOCORRELATION FUNCTION

The choice of an appropriate form for the acfs was dictated not only by the necessity to fit the data, but also by the following *a priori* considerations:

- (a) The restrictions upon and relations between the acfs of geopotential and wind components at zero time lag have been discussed by Buell (1972a) for geostrophic flow in a horizontally homogeneous and isotropic atmosphere. To the extent that these conditions apply over limited geographical areas in the real atmosphere,  $r_u$  and  $r_v$  are constrained to forms which are consistent with

each other and a permissible form of geopotential acf. An additional consequence of the above assumptions is that  $r_u$  and  $r_v$  at zero time lag depend strongly on the direction as well as the magnitude of separation, a feature which has been confirmed by many observational studies.

- (b) At non-zero time lags,  $r(x, y, t)$  should be a maximum in the x-y plane at a displacement from the origin in the usual direction of movement of perturbations to the mean flow. If the frozen turbulence hypothesis of Taylor (1938) were applicable to the macroscale, the displacement should correspond to the travel of the mean wind during the time lag. Buell (1972b) found that frozen turbulence was not verified at the 500 mb level over North America for time lags from 1 to 3 days. Spillane (1969) has also cast doubt on its validity at 200 and 300 mb over Australia for lags up to 48 hours.

The maximum value in the x-y plane of  $r(x, y, t)$  should decrease with increasing lag, due to the increasing effect of evolutionary processes, and the increasing scatter in the movement of perturbations.

- (c) Correlation coefficients obtained from observed winds will underestimate the true value because of observational error and small scale noise. For a random error variance of  $\sigma_\epsilon^2$ , the true and observed correlation coefficients  $r$  and  $\hat{r}$  are related by

$$r = \hat{r} \left( 1 + \frac{\sigma_\epsilon^2}{\sigma^2} \right)$$

where  $\sigma^2$  is the true variance.

## MANUALLY DRAWN CONTOURS

Correlation coefficients of each component for all station pairs (P and P') were stratified by level, season and time lag. The lagging member (P) of each pair was located at the origin of a cartesian set of axes, and the values of  $r_u$  and  $r_v$  were plotted at the location (x, y) of P'. Smooth manual contours of  $r(x, y)$  were drawn, as in Figs 1(a) to 1(d). At zero lag, values of  $r_u$  and  $r_v$  were plotted twice, with each member at the origin. The assumption implicit in this procedure is that the values of  $r_u$  and  $r_v$  are dependent upon the space-time *separation* of a station pair and not upon the space-time location of either member.

At zero lag, although there was qualitative agreement with homogeneous, isotropic, geostrophic theory, there was considerable scatter in the observed data, and two systematic discrepancies. Particularly at 200 mb, the values of  $r_u$  decreased more rapidly in the north-south direction than did the values of  $r_v$  in an east-west direction, although the theory predicts the same rate of decrease. Also, the elongated contours of  $r_u$  and  $r_v$  were oriented not exactly in the east-west and north-south directions as predicted by theory, but were slightly rotated towards a north-west-southeast orientation. With increasing time lag, the maxima of  $r_u$  and  $r_v$  in the x-y plane showed systematic movement from the origin, although the displacement was much less than that predicted by frozen turbulence. There is obviously insufficient data at large spatial separation to define adequately the negative lobes.

## FITTING OF AUTOCORRELATION FUNCTIONS

In view of the gross correspondence of the manual contours at zero lag to homogeneous, isotropic, geostrophic flow, it was decided to constrain the forms of acfs accordingly, and the following were selected:

$$r_u(x,y,t) = c_u (1-\beta^2(y-Vt)^2) \exp(-0.5\beta^2((x-Ut)^2+(y-Vt)^2)) \exp(-0.5\alpha_u^2 t^2)$$

$$r_v(x,y,t) = c_v (1-\beta^2(x-Ut)^2) \exp(-0.5\beta^2((x-Ut)^2+(y-Vt)^2)) \exp(-0.5\alpha_v^2 t^2)$$

where  $c_u$ ,  $c_v$ ,  $\alpha_u$ ,  $\alpha_v$ ,  $\beta$ ,  $U$  and  $V$  are constants to be determined by the data.

At zero time lag, these forms are consistent with a geopotential acf of the traditional Gaussian form (see Buell 1972a, Table 1, Index 1).

$$r_h = \exp(-0.5 \beta^2 \rho^2)$$

where  $\rho^2 = x^2 + y^2$ . The constants  $c_u$  and  $c_v$  account for random observational error, and  $U$  and  $V$  are components of an advecting wind corresponding to the movement of the maximum correlation centre with increasing time lag.  $\alpha_u$  and  $\alpha_v$  account for the decrease with time lag of the central maxima. Conceptually, it is easy to associate  $U$  and  $V$  with the movement of perturbations to the mean flow, and  $\alpha_u$ ,  $\alpha_v$  with evolutionary processes. However, for reasons suggested in the last sentence of (b) on page 28 above, and elaborated in later discussion, the effects of movement and evolution cannot be separated completely.

A surface fitting algorithm developed by Nelson (1969) was used to determine the constants. This is an iterative technique combining the Gaussian (Taylor series) method and the method of steepest descent at each iteration.

The use of constant advecting wind components  $U$  and  $V$  assumes that the maximum correlation centre moves at uniform speed for time lags up to 24 hours. This was verified by comparing error residuals corresponding to a uniform speed, with residuals resulting from an individual fitting at each time lag. The error variance reductions in the latter cases were non-significant on the basis of standard F tests.

## RESULTS AND DISCUSSION

Functions were fitted to 16 subsets of the correlation coefficients (2 levels, 2 seasons, 4 parent stations) and to combinations of the subsets. Values of the fitted constants, together with residual RMS errors, are shown in Table 1. Contours of the fitted acf, comparable with Figs 1(a) to 1(d), are illustrated in Figs 2(a) to 2(d).

The chosen form of acf explains approximately 85 per cent of the variance in the basic correlation coefficient data, with a typical RMS residual of 0.12. Standard F tests indicated that for many of the subsets, use of the acf for the particular subset resulted in a significantly lower residual variance (95% confidence level) than did the acf for combined seasons, levels or stations.

The functions naturally fail to account for the discrepancies from theory noted above under 'manually drawn contours'. They also systematically underestimate the observed values close to the origin for time lags up to 12 hours. A contributory factor is probably the random error assumption (implicit in the constants  $c_u$  and  $c_v$ ) which, among other things, fails to account for the bias and selectivity introduced by the mixture of radar and pilot balloon winds in the basic data. A choice of component acfs based on a geopotential acf other than the simple Gaussian might also ameliorate this deficiency. For 500 mb winter geopotential data over North America, Julian and Thiebaut (1975) have shown that several functional forms fit the data slightly better than the Gaussian acf.

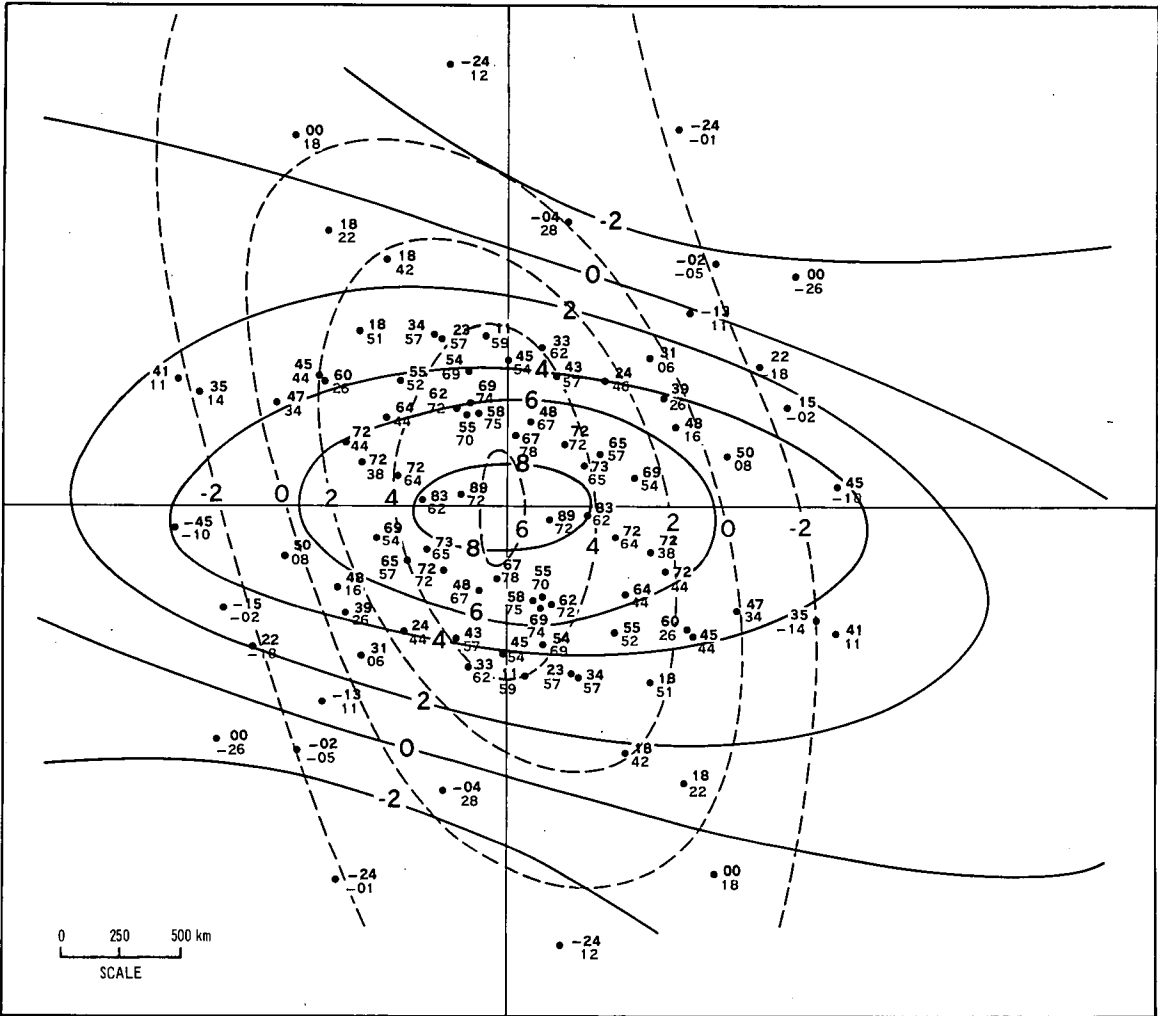


Fig 1(a) Manually drawn contours of  $r_U(x, y, t)$  - full lines, and  $r_V(x, y, t)$  - dashed lines, at  $t=0$  hours; all stations combined, 500 mb, winter. Observed values of  $r_U$  (upper) and  $r_V$  (lower) are shown. The preceding decimal point has been omitted from both the contours and the observed values.

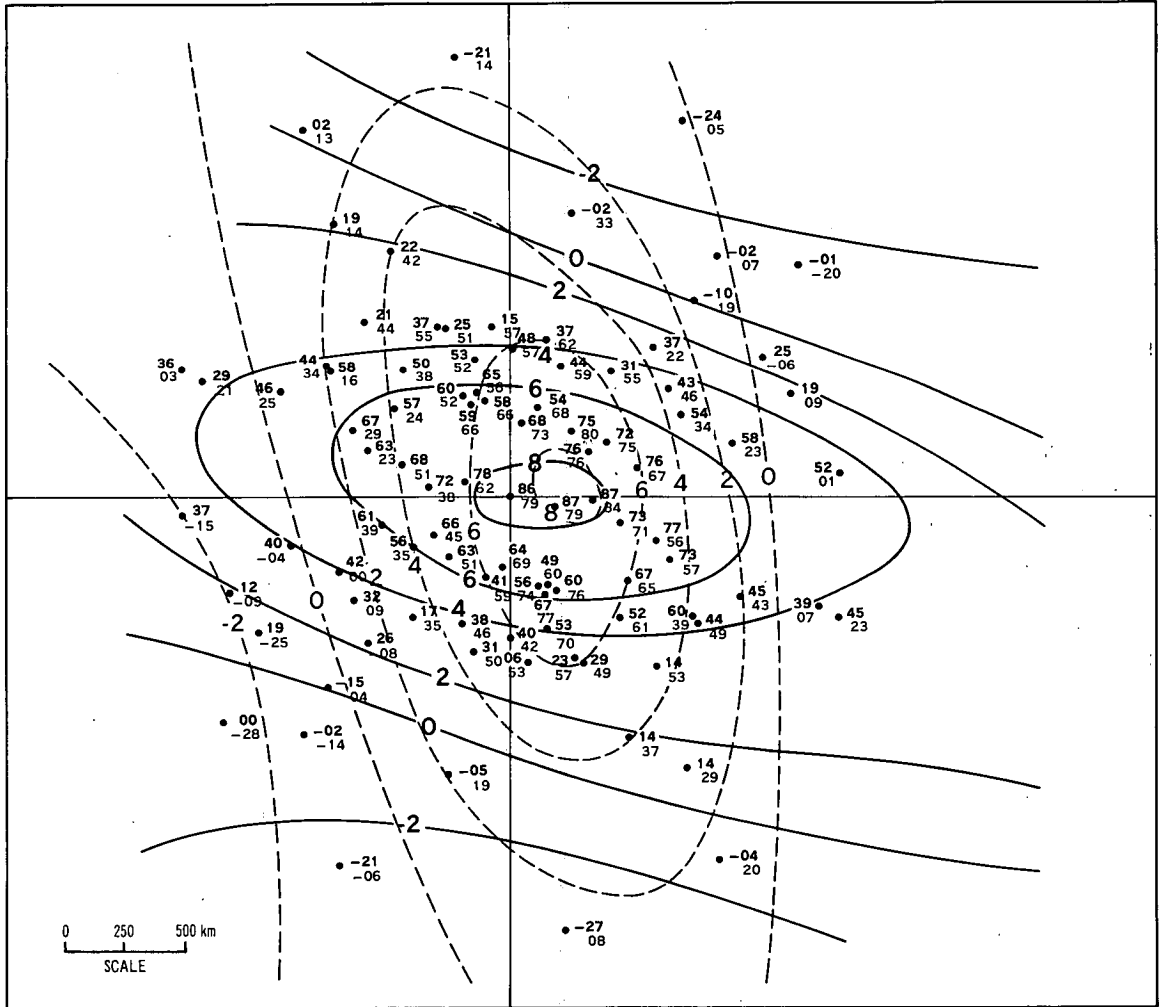


Fig 1(b) Manually drawn contours of  $r_U(x, y, t)$  – full lines, and  $r_V(x, y, t)$  – dashed lines, at  $t=6$  hours; all stations combined, 500 mb, winter. Observed values of  $r_U$  (upper) and  $r_V$  (lower) are shown. The preceding decimal point has been omitted from both the contours and the observed values. Lag is relative to station at origin.

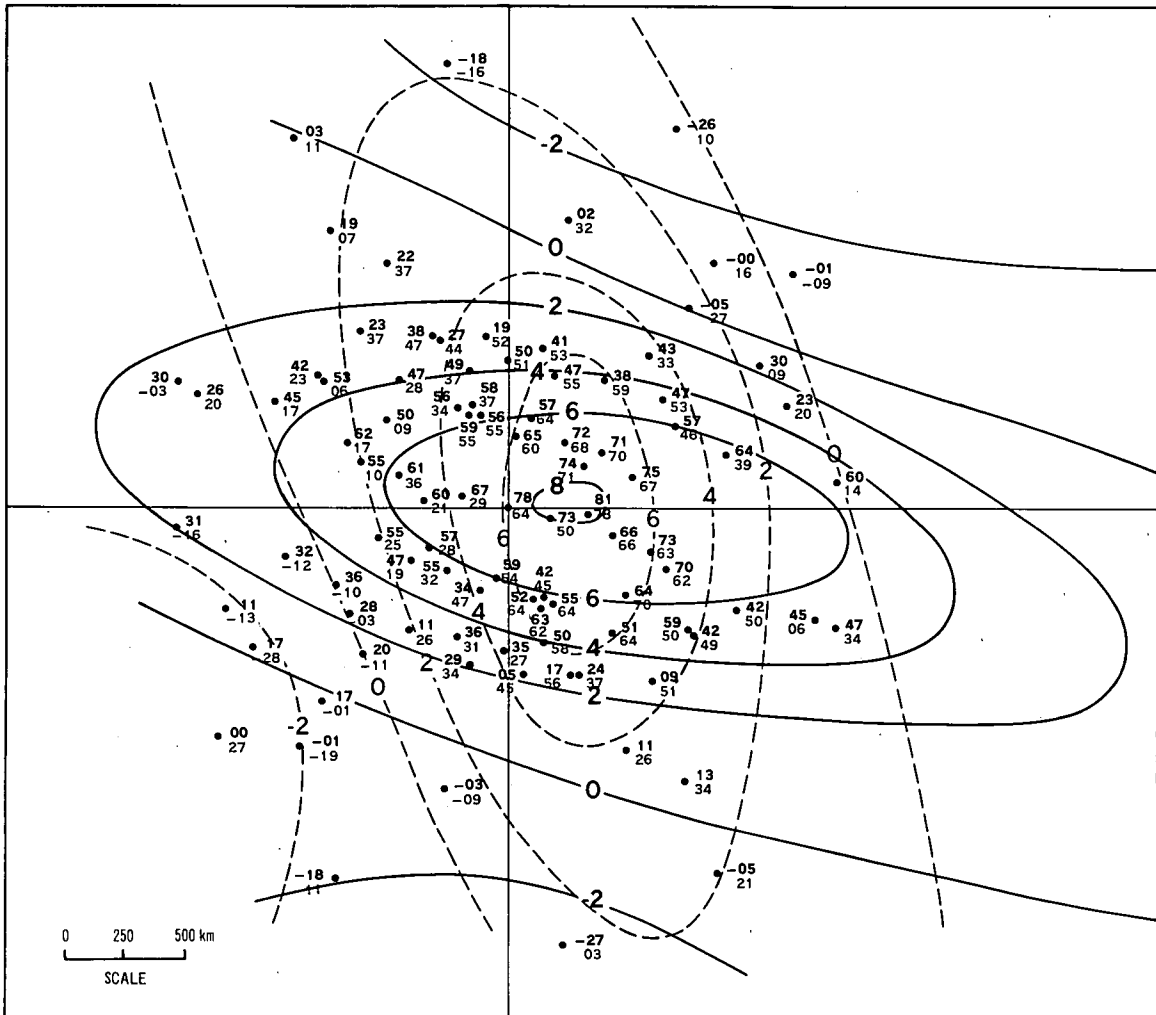


Fig 1(c) Manually drawn contours of  $r_u(x, y, t)$  – full lines, and  $r_v(x, y, t)$  – dashed lines, at  $t=12$  hours; all stations combined, 500 mb, winter. Observed values of  $r_u$  (upper) and  $r_v$  (lower) are shown. The preceding decimal point has been omitted from both the contours and the observed values.

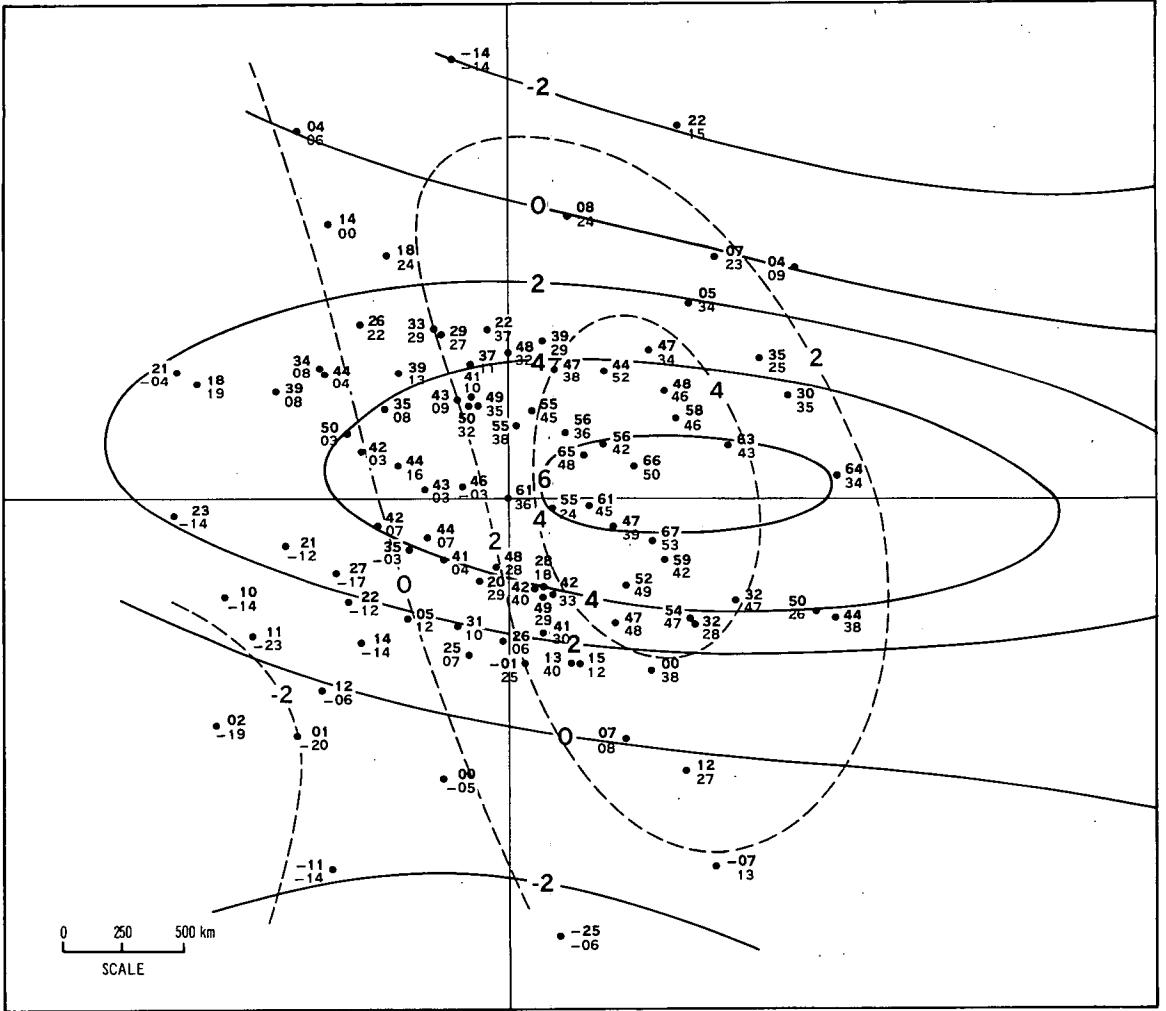


Fig 1(d) Manually drawn contours of  $r_{II}(x, y, t)$  – full lines, and  $r_V(x, y, t)$  – dashed lines, at  $t=24$  hours; all stations combined, 500 mb, winter. Observed values of  $r_{II}$  (upper) and  $r_V$  (lower) are shown. The preceding decimal point has been omitted from both the contours and the observed values.

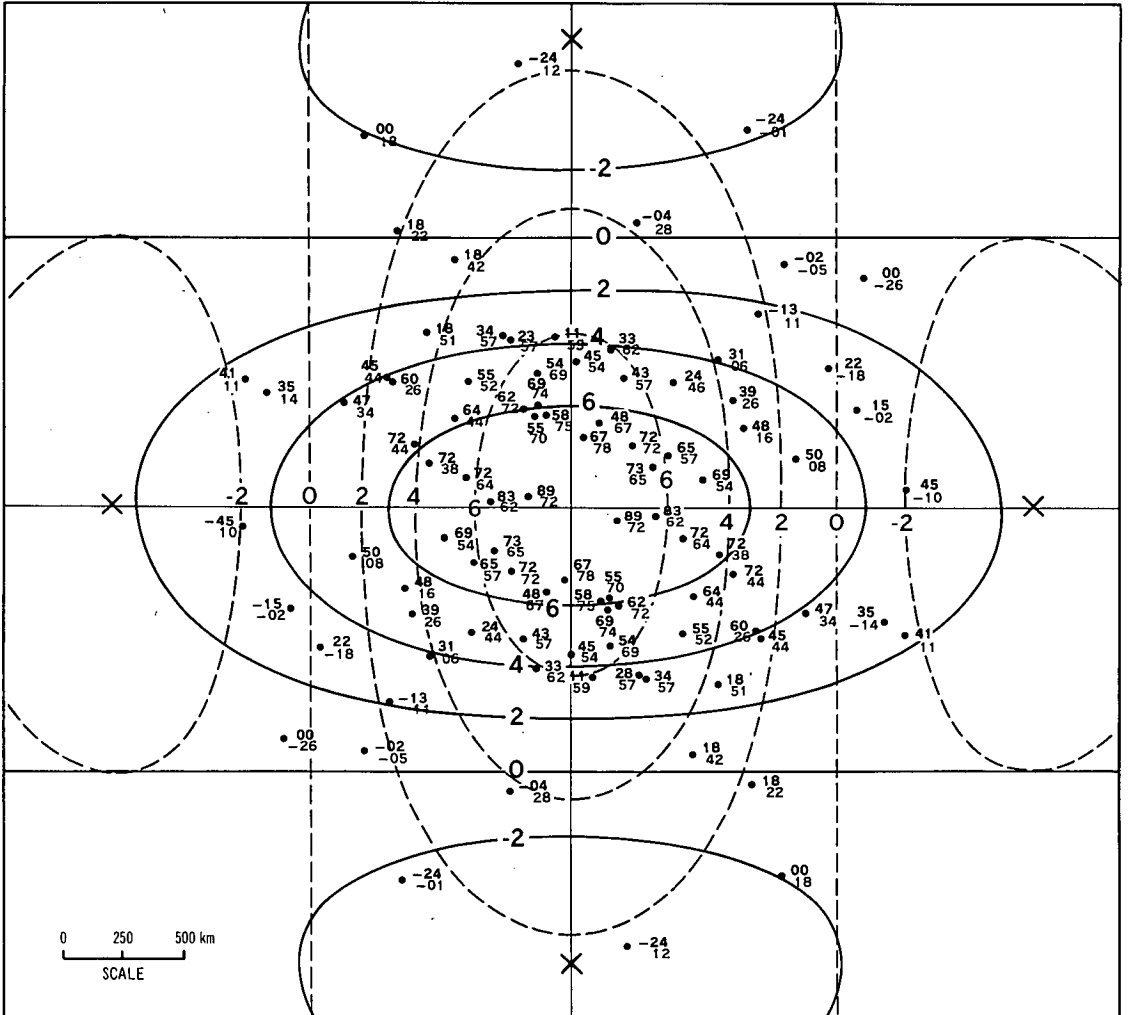


Fig 2(a) Fitted autocorrelation functions  $r_U(x, y, t)$  and  $r_V(x, y, t)$  at  $t=0$  hours; all stations combined, 500 mb, winter. Observed values of  $r_U$  (upper) and  $r_V$  (lower) are shown. The preceding decimal point has been omitted from both the contours and the observed values.

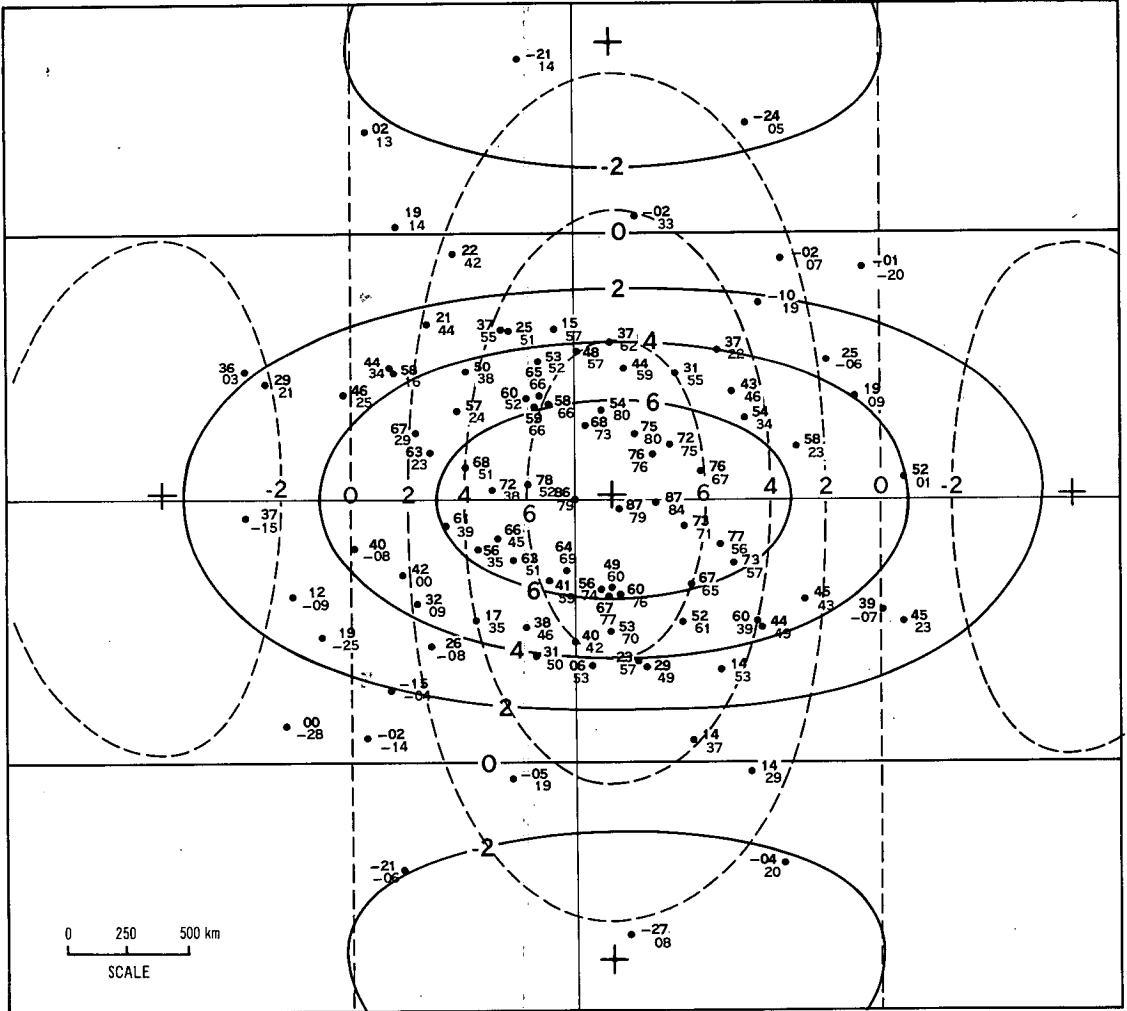


Fig 2(b) Fitted autocorrelation functions  $r_U(x, y, t)$  and  $r_V(x, y, t)$  at  $t=6$  hours; all stations combined, 500 mb, winter. Observed values of  $r_U$  (upper) and  $r_V$  (lower) are shown. The preceding decimal point has been omitted from both the contours and the observed values. Lag is relative to station at origin.

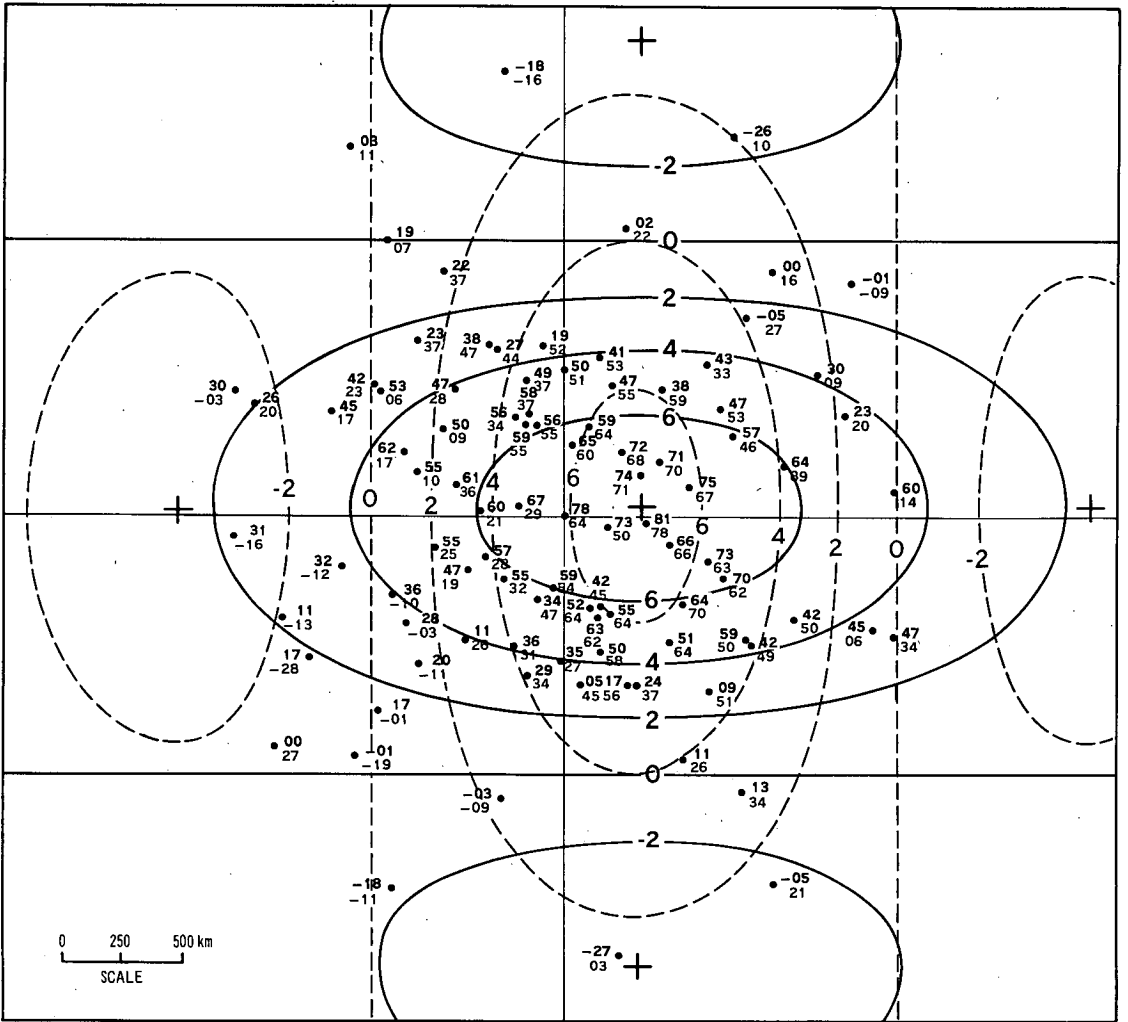


Fig 2(c) Fitted autocorrelation functions  $r_U(x, y, t)$  and  $r_V(x, y, t)$  at  $t=12$  hours; all stations combined, 500 mb, winter. Observed values of  $r_U$  (upper) and  $r_V$  (lower) are shown. The preceding decimal point has been omitted from both the contours and the observed values.

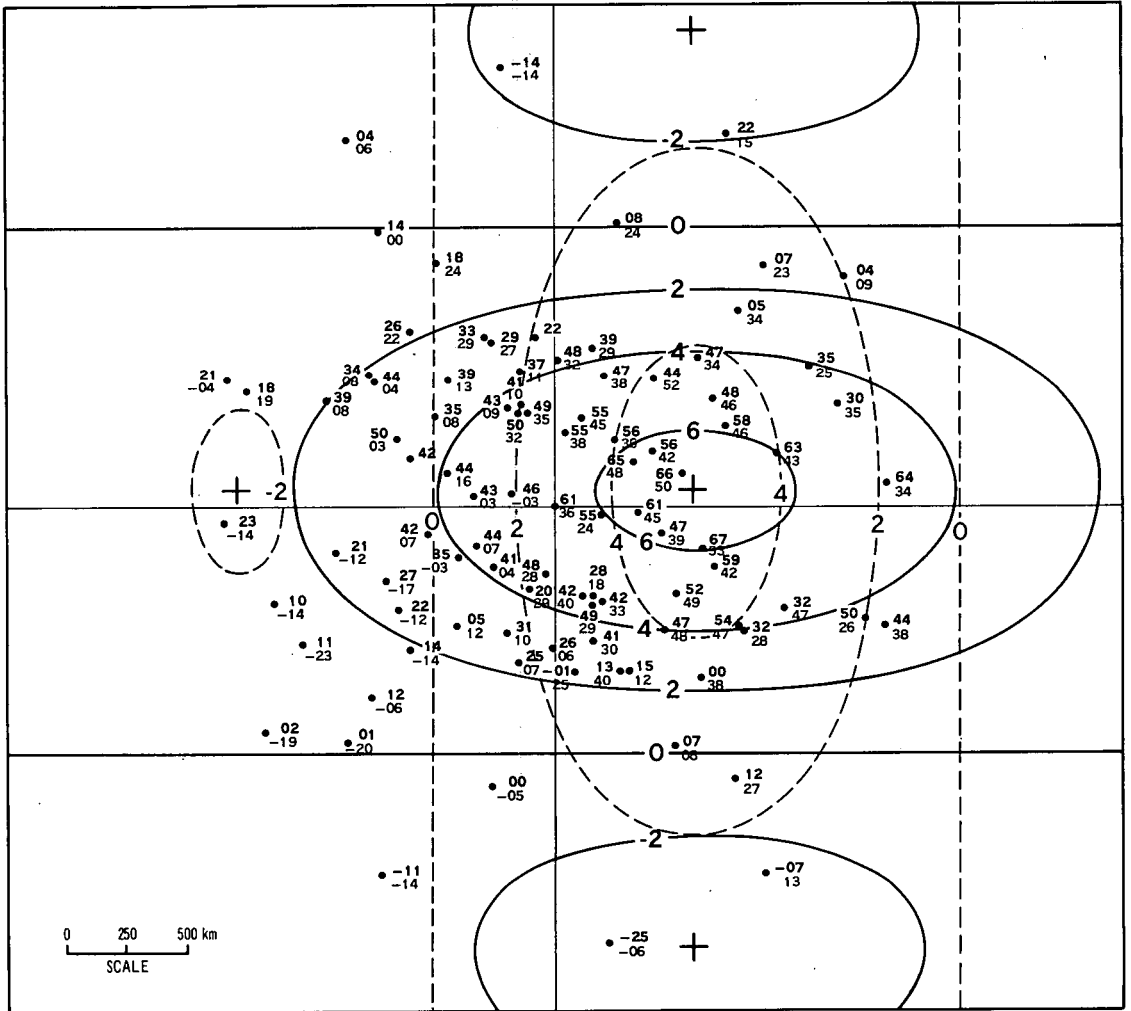


Fig 2(d) Fitted autocorrelation functions  $r_U(x, y, t)$  and  $r_V(x, y, t)$  at  $t=24$  hours; all stations combined, 500 mb, winter. Observed values of  $r_U$  (upper) and  $r_V$  (lower) are shown. The preceding decimal point has been omitted from both the contours and the observed values.

Table 1 Autocorrelation function constants for the 16 subsets and various combinations. N is the number of correlation coefficient values used, E is the residual RMS error, and the other constants are defined in the text. Units are  $\alpha$ -hr $^{-1}$ ;  $\beta$ -km $^{-1}$ ; U, V-km hr $^{-1}$ .

Station	Giles (25°02'S, 128°18'E)				Eagle Farm (27°26'S, 153°05'E)				Laverton (37°52'S, 144°45'E)				Carnarvon (24°53'S, 113°39'E)				All stations				
	Season	Winter	Summer	200	500	Winter	Summer	200	500	Winter	Summer	200	500	Winter	Summer	200	500	Winter	Summer	200	500
N	73	73	73	73	101	101	101	101	108	108	108	108	108	80	80	80	80	362	362	362	362
C <sub>u</sub>	0.63	0.73	0.77	0.78	0.76	0.81	0.86	0.83	0.90	0.78	0.89	0.85	0.63	0.60	0.80	0.78	0.77	0.76	0.83	0.82	0.82
C <sub>v</sub>	0.80	0.70	0.71	0.62	0.91	0.77	0.87	0.77	0.82	0.73	0.80	0.74	0.84	0.70	0.74	0.66	0.85	0.74	0.78	0.71	0.71
$\alpha_u(\times 10^{-2})$	1.8	1.9	1.3	1.9	2.4	2.0	1.9	2.1	2.2	2.2	2.5	2.7	1.6	2.3	2.0	2.2	2.3	2.3	2.3	2.5	2.5
$\alpha_v(\times 10^{-2})$	2.7	3.6	2.9	2.9	3.0	3.5	2.7	3.0	3.9	3.5	3.9	3.9	3.0	4.1	3.4	3.7	3.4	3.9	3.6	3.8	3.8
$\beta(\times 10^{-3})$	0.71	0.83	0.80	0.90	0.93	0.94	1.0	0.97	0.89	0.84	1.0	0.93	0.77	0.78	0.85	0.91	0.86	0.88	0.92	0.93	0.93
U	25	25	3.7	5.2	21	22	6.6	7.6	28	35	17	21	19	23	3.2	4.2	23	26	8.3	9.2	9.2
V	14	7.5	2.2	2.0	4.5	4.1	3.2	3.6	4.2	2.4	2.9	2.0	12	5.1	1.2	-1.1	7.1	4.1	2.5	1.6	1.6
E	0.11	0.12	0.15	0.07	0.11	0.09	0.12	0.06	0.09	0.08	0.09	0.07	0.13	0.15	0.11	0.09	0.12	0.11	0.13	0.08	0.08

	Combined levels and seasons				Combined stations and seasons				Combined levels and seasons			
	Giles Farm	Eagle Farm	Laverton	Carnarvon	200 mb	500 mb	200 mb	500 mb	Summer	Summer	Summer	Summer
N	292	404	432	320	724	724	724	724	724	724	724	724
C <sub>u</sub>	0.72	0.81	0.85	0.71	0.80	0.79	0.80	0.83	0.83	0.83	0.83	0.77
C <sub>v</sub>	0.71	0.83	0.77	0.74	0.82	0.72	0.82	0.75	0.75	0.75	0.80	0.80
$\alpha_u(\times 10^{-2})$	1.9	2.2	2.5	2.3	2.4	2.5	2.4	2.4	2.4	2.4	2.3	2.3
$\alpha_v(\times 10^{-2})$	3.3	3.3	3.9	3.8	3.7	4.1	3.7	3.7	3.7	3.7	3.7	3.7
$\beta(\times 10^{-3})$	0.81	0.97	0.92	0.84	0.89	0.90	0.89	0.93	0.93	0.93	0.87	0.87
U	14	14	25	12	15	17	15	8.7	8.7	8.7	24	24
V	5.7	3.8	2.8	3.8	4.5	2.9	4.5	2.1	2.1	2.1	5.6	5.6
E	0.13	0.11	0.09	0.14	0.13	0.10	0.13	0.11	0.11	0.11	0.12	0.12

Nevertheless, Table 1 still yields some apparently significant information. For all the subsets,  $\alpha_v$  is greater than  $\alpha_u$ , reflecting the fact that the maximum of  $r_v$  in the x-y plane decreases more rapidly with increasing time lag than does the maximum of  $r_u$ . Because of the association of U and V with perturbation movement, and  $\alpha_u$ ,  $\alpha_v$  with evolution, it might be tempting to conclude that, in a quasi-Lagrangian system following a perturbation, the meridional component undergoes more rapid evolution than does the zonal. However, the relative magnitudes of  $\alpha_u$  and  $\alpha_v$  can be explained without postulating different evolutionary properties for the two components. The values of U and V, and independent synoptic experience, indicate that the usual direction of perturbation movement is approximately west to east, and the location of the point of maximum correlation is close to the zonal axis. Let the location M of the correlation maximum at lag  $\tau$  be  $(x_\tau, y_\tau)$ , with  $y_\tau \ll x_\tau$ . In a specific synoptic situation, the end point of the displacement of a perturbation during lag  $\tau$  will probably be either to the east or to the west of M. Overall, the value of  $r_u$  (or  $r_v$ ) at M will therefore result from an ensemble of situations in which M is located in an approximately zonal direction from the perturbation centre. The respective contours of  $r_u$  and  $r_v$  at zero lag indicate that  $r_v$  decreases more rapidly in the zonal direction than does  $r_u$ . At all lags  $\tau$ ,  $r_v(x_\tau, y_\tau)$  will therefore be less than  $r_u$ . Consequently  $\alpha_v$  will be greater than  $\alpha_u$ . While the relative magnitudes of  $\alpha_v$  and  $\alpha_u$  can be explained in this way, the possibility remains that a similar effect could also have been caused by a systematic bias in the basic wind data differently affecting  $r_u$  and  $r_v$ . It is interesting that Buell's (1972b) North American data at 24 hour lag indicate the reverse situation to ours, with  $r_v(x_\tau, y_\tau)$  slightly greater than  $r_u$ .

The constant  $\beta$  defines a scale parameter  $L = \beta^{-1}$  which is the distance at which the transverse correlation coefficient first becomes zero. For zonal and meridional coefficients, it is the distance to the first zero of  $r_u$  in the north-south direction and of  $r_v$  in the west-east direction. The range of  $\beta$  for the different subsets corresponds to a range of L from 1000 to 1300 km. As implied under 'manually drawn contours' above, discrepancies from theory indicate a somewhat larger value of L for the meridional component and smaller value for the zonal. Julian and Thiebaux (1975) have noted similar behaviour in 500 mb winter wind data over North America.

There is a pronounced contrast between seasons in respect of the constants U and V, at both levels and at all stations, particularly at Giles and Carnarvon. In both seasons but particularly in summer, and at both levels, the resultant speed  $(U^2 + V^2)^{1/2}$  at Laverton is greater than at the other stations. These are not unexpected results, in view of the association of U and V with the velocity of perturbations to the mean flow. The values of U and V at Laverton for 500 mb, averaged over seasons, correspond to a 24 hour displacement of about 700 km, which agrees closely with Buell's (1972b) data at similar latitudes. There appears to be no systematic difference in the values of U and V at the two levels.

For certain applications (eg, objective analyses, space-time data assimilation, multiple linear regression predictions) it may be desirable to reduce the number of different constants for the various seasons, levels, and geographical areas. A reasonable approximation would be to allow U and V to vary with latitude and season, and to use invariant values of the other constants. In any case, the acfs should not be applied at lags much beyond 24 hours. If the application does not necessitate a homogeneous, isotropic and geostrophic constraint, an attempt could also be made to account for the systematic discrepancies from theory mentioned above.

## ACKNOWLEDGMENT

Thanks are extended to Mrs S. Ickeringill for data preparation.

## REFERENCES

- Buell, C.E. 1971. Two-point wind correlations on an isobaric surface in a non-homogeneous non-isotropic atmosphere. *Jnl appl. Met.*, 10, 1266-1274.
- Buell, C.E. 1972a. Correlation functions for wind and geopotential on isobaric surfaces. *Jnl appl. Met.*, 11, 51-59.
- Buell, C.E. 1972b. Variability of wind and distance and time on an isobaric surface. *Jnl appl. Met.*, 11, 1085-1091.
- Julian, P.R. and Thiebaux, H.J. 1975. On some properties of correlation functions used in optimum interpolation schemes. *Mon. Weath. Rev.*, 103, 605-616.
- Nelson, H.W. 1969. *Computer Non Linear Least Squares Regression Program*. IBM Contributed Library.
- Seaman, R.S. and Draudins, I.M. 1975. Statistics on the simultaneous variation of wind in time and space - Australian region, 20 000 and 40 000 ft. *ANMRC Tech. Rep. 1*.
- Spillane, K.T. 1969. Synoptic and structural analysis of TOPCAT flight situations. Project TOPCAT, *Met. Report XII*, University of Melbourne.
- Taylor, G.I. 1935. Statistical theory of turbulence Part 1. *Proc. Roy. Soc., A*, 151, 421-444.